How Many-Body Effects Modify the van der Waals Interaction between Graphene Sheets

John F. Dobson,[1,2,3,*] Tim Gould,[1] and Giovanni Vignale[3]

[1]*Queensland Micro and Nano Technology Centre, Griffith University, Nathan, Queensland 4111, Australia*

[2]*Donostia International Physics Centre and European Theoretical Spectroscopy Centre, Universidad del Pais Vasco, San Sebastian, 2008, Spain*

[3]*Department of Physics, University of Missouri, Columbia, Missouri 65211, USA*

(Received 20 June 2013; published 29 May 2014)

Undoped-graphene (Gr) sheets at low temperatures are known, via random-phase-approximation (RPA) calculations, to exhibit unusual van der Waals (vdW) forces. Here, we show that graphene is the first known system where effects beyond the RPA within each interacting subsystem make qualitative changes to the vdW force, observable via its local exponent $d\log(F)/d\log(D)$. For large separations $D \gtrsim 10$ nm, where only the π_z vdW forces remain, we find that the Gr-Gr vdW interaction is substantially reduced from the RPA prediction. Its D dependence is very sensitive to the form of the long-wavelength, in-plane many-body enhancement of the velocity of the massless Dirac fermions and may provide independent confirmation of the latter via direct force measurements. The simple connection that we expose is a strong motivation for further refinement of recent successful direct vdW force measurements.

DOI: 10.1103/PhysRevX.4.021040

Subject Areas: Computational Physics, Condensed Matter Physics, Graphene, Quantum Physics

I. INTRODUCTION

It is well known that a zero-gap conical π_z electronic Bloch band structure of undoped graphene, supporting massless Dirac fermions propagating with speed v, should give this system a number of unusual properties [1]. One such property relates to the low-temperature dispersion [van der Waals (vdW)] interaction energy per unit area E^{vdW}/A between parallel undoped-graphene sheets separated by a large distance D. Commonly used theories, such as the summation of pairwise atomic contributions $E^{\mathrm{vdW}} \approx \sum_{i\neq j} C_{ij} R_{ij}^{-6}$ and other popular and largely successful approaches [2–6], predict the energy for this case (and any case with parallel 2D sheet geometry) to be a power law

$$\frac{E^{\mathrm{vdW}}}{A} = -\frac{C_4}{D^4}, \tag{1}$$

where C_4 is a system-dependent constant. (See Secs. 4 and 8 of Ref. [7] for further discussion.) By contrast, more microscopic or collective approaches, such as the random-phase-approximation (RPA) correlation energy based on the graphene π_z-π_z^* electronic response, yield the result [8–12]

$$\frac{E^{\mathrm{vdW}}}{A} = -\frac{C_3}{D^3}. \tag{2}$$

RPA-like approaches also predict interesting beyond-pairwise effects [13] even outside the asymptotic large-D regime.

The constant C_3 in Eq. (2) is easily calculated within the RPA, which treats the electrons in each layer as essentially noninteracting but subjected to their own time-dependent classical electrostatic field. Indeed, if one makes the simplest ("Casimir-Polder") approximation, in which the interlayer Coulomb interaction is treated by second-order perturbation theory, one finds, in the limit of large separation,

$$C_3 = \frac{e^2}{32\pi} F\left(\frac{\pi}{2}\alpha\right), \tag{3}$$

where $\alpha = (e^2/\hbar v)$ is the effective fine-structure constant of graphene, related to the velocity v of the massless Dirac fermions as the fundamental fine-structure constant is to the speed of light, and $F(a)$ is a smoothly varying function, which is plotted in Fig. 1. [The derivation of this result, as well as the analytic expression for $F(a)$, will be presented below.] For $v = 10^6$ m/s, one has $\alpha \simeq 2.2$, which makes C_3 very close to the "universal" value $C_3^{\mathrm{uni}} = (e^2/32\pi)$. This value is weakly dependent on small variations of v, and remarkably, the interaction $-C_3^{\mathrm{uni}}/D^3$ is not changed by the inclusion of electromagnetic retardation, even at large D values. [See Eq. (36) of Refs. [14,15] and Eq. (8b) of Ref. [8] corrected for a spurious factor of 2.]

*Corresponding author.
j.dobson@griffith.edu.au

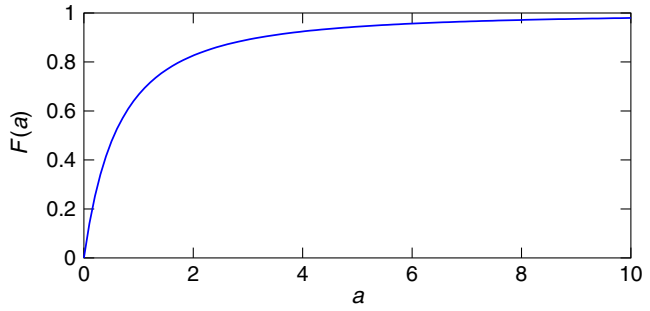

FIG. 1. Plot of the function F that controls, via Eq. (3), the value of the constant C_3 for the RPA van der Waals interaction between graphene sheets.

In this context, it is important to note that for real graphene, Eq. (2) is valid only at large separations: At shorter distances, gapped transitions other than the $\pi_z \to \pi_z^*$ contribute a vdW energy of the conventional form [Eq. (1)]. It is only for $D \gtrsim 10$ nm that numerical work within the RPA [16] suggests that the D^{-3} falloff overtakes the conventional D^{-4} contribution. It is, therefore, in this regime of larger separations corresponding to small wave vectors that one should check for any many-body effects beyond the RPA due to the π_z-π_z^* graphene response. Furthermore, at these separations, all electrostatic and metallic overlap forces have long vanished.

II. RENORMALIZATION OF THE VELOCITY

Such corrections are worth investigating because the π_z electrons in a graphene sheet are obviously not "weakly interacting": The coupling constant α is larger than 1 [17–21]. What is believed to be true is that the effective long-wavelength Hamiltonian, generated by a renormalization-group (RG) flow, is noninteracting [17,18,22–24]. However, the reason for this simplification is not that the electric charge renormalizes to 0 but that the fermion velocity grows to infinity. More precisely, if one introduces an effective fermion velocity v_q, which describes the system at length scales larger than $1/q$, then $v_q \to \infty$ for $q \to 0$, and, accordingly, the running coupling constant $\alpha_q = (e^2/\hbar v_q)$ tends to 0.

This long-wavelength renormalization is quite distinct from beyond-RPA corrections at short wavelengths, arising from semilocal modifications of the adiabatic local-density approximation of time-dependent density-functional theory, which are also sometimes described as "renormalized" [25]. Our long-wavelength corrections can change the asymptotic power law for the van der Waals interaction, whereas the short-ranged adiabatic local-density-approximation-based ones, unsurprisingly, have no major qualitative effect on long-wavelength vdW phenomena [26]. Indeed, we suspect that the renormalized theories used here could be related to a highly nonlocal form of the time-dependent density-functional-theory exchange-correlation kernel.

The stronger the original interaction is at the microscopic scale, the larger the renormalized velocity becomes at any given length scale $1/q$. The exact form of the divergence of v_q for $q \to 0$ is, of course, unknown, since the many-body problem has not been solved. RG calculations based on first-order perturbation theory [17,24] suggest a weak logarithmic divergence of the form

$$v_q^{(1)} = v\left(1 + \frac{1}{4}\alpha \ln\frac{\Lambda}{q}\right), \qquad \alpha_q^{(1)} = \frac{\alpha}{1 + \frac{1}{4}\alpha \ln\frac{\Lambda}{q}}, \tag{4}$$

where Λ is a microscopic cutoff of the order of the inverse of the lattice constant (Å). More sophisticated calculations at the "two-loop" level and in the large-N limit [18,24,27–31], N being the number of fermion flavors, predict a stronger power-law divergence of the form

$$v_q^{(2)} = v\left(\frac{\Lambda}{q}\right)^{\beta}, \qquad \alpha_q^{(2)} = \frac{\alpha}{(\Lambda/q)^{\beta}}, \tag{5}$$

where $\beta = (8/N\pi^2)$. ($N = 4$ for graphene.) Recent experiments performed by a variety of techniques have at least partially confirmed these theoretical predictions [19–21,32], showing that the effective coupling constant is reduced and the Dirac cones are strongly compressed [20] near the Dirac point.

The many-body enhancement of the fermion velocity has also been shown to affect various many-body phenomena, such as the plasmon dispersion [33,34], the optical Drude weight [33], and the electronic screening of external charges [35]. To date [25,26], beyond-RPA effects were believed to alter at most the prefactor, not the power exponent, of vdW decay with distance. In this article, we expose a striking case where beyond-RPA many-body renormalization affects the essential character of a vdW interaction, namely, that between graphene sheets. Our main result is that the long-wavelength enhancement of the fermion velocity causes the vdW interaction to decrease asymptotically faster than in Eq. (2) but still slower than in the conventional Eq. (1). This result can be expressed in an intuitively appealing way by saying that the bare α in Eq. (3) must be replaced by the running coupling constant α_q evaluated at $q = 1/D$. Thus, we have

$$\frac{E^{\mathrm{vdW}}}{A} \simeq -\frac{e^2}{32\pi D^3} F\left(\frac{\pi}{2}\alpha_{1/D}\right), \tag{6}$$

and since $F(x) \simeq (\pi/2)x$ for $x \ll 1$, the asymptotic behavior of the vdW interaction is reduced, relative to the RPA, by a factor proportional to $\alpha_{1/D}$, which vanishes in the limit $D \to \infty$. The renormalized interaction will therefore decrease as $[D^3 \ln(D\Lambda)]^{-1}$ or as $D^{-(3+\beta)}$, depending on which of the two scenarios, Eq. (4) or Eq. (5), is realized. Additional many-body effects contained in the so-called vertex corrections turn out to be irrelevant at sufficiently

large distances, even though, of course, they can quantitatively change the result at intermediate distances. Throughout the analysis, we assume that the distances are not so large that $v_{q=1/(2D)}$ becomes comparable to the speed of light, at which point electromagnetic retardation effects should be taken into account. Using this criterion, retardation becomes dominant only for D of order 10^{220} m for the logarithmic renormalization case [Eq. (4)] or $O(10^1$ m) for the power-law case [Eq. (4)]. Thus, retardation here is unimportant in practice, as for the pure RPA theory.

III. VAN DER WAALS CALCULATIONS

We consider the interaction energy between two parallel freely suspended graphene sheets *in vacuo*, separated by a distance D that is much larger than the two-dimensional lattice constant a, as well as the thickness T of each sheet. (See the Appendix for other scenarios.) Our starting point is the Casimir-Polder formula obtained by doing straightforward second-order perturbation theory in the interlayer electron-electron interaction potential

$$V_{\text{inter}}(q) = \frac{2\pi e^2}{q} e^{-qD}, \tag{7}$$

where $\mathbf{q}$ is the two-dimensional wave vector of density fluctuations in each layer. The result is

$$\frac{E^{(2)}}{A} = \frac{-\hbar}{8\pi^3} \int_0^\infty du \int d^2\mathbf{q} \chi(q, iu)^2 \left(\frac{2\pi e^2}{q} e^{-qD}\right)^2. \tag{8}$$

Here, $\chi(q, iu)$ is the electronic density-density response function of a single isolated layer, evaluated at wave vector $\mathbf{q}$ and imaginary frequency iu. The exponentially decaying factor $\exp(-2qD)$ ensures that small wave vectors $q \approx 1/D$ dominate Eq. (8) for large separations.

The response function $\chi(q, iu)$ is expressed in terms of the proper response function $\tilde{\chi}(q, iu)$ and the intralayer interaction potential $V_{\text{intra}}(q) = (2\pi e^2/q)$ according to the well-known formula [36]

$$\chi(q, iu) = \frac{\tilde{\chi}(q, iu)}{1 - \frac{2\pi e^2}{q}\tilde{\chi}(q, iu)}. \tag{9}$$

In the RPA, one approximates $\tilde{\chi}(q, iu) \approx \chi_0(q, iu)$, where

$$\chi_0(q, iu) = -\frac{1}{4\hbar v} \frac{q}{\sqrt{1 + x^2}} \tag{10}$$

is the noninteracting zero-temperature response function for the conical π_z bands [8,17,37], v is the bare velocity, and $x \equiv (u/qv)$.

Intralayer electron-electron interactions modify $\tilde{\chi}$ in two ways: via self-energy insertions and via vertex corrections. For example, in a recent first-order perturbative calculation coupled with RG arguments, Sodemann and Fogler have found [35]

$$\tilde{\chi}(q, iu) = -\frac{q}{4\hbar v_q} \left(\frac{1}{\sqrt{x_q^2 + 1}} + \alpha_q J(x_q)\right), \tag{11}$$

where $x_q = u/(qv_q)$ with v_q given by Eq. (4) (i.e., $v_q = v_q^{(1)}$) and α_q is the corresponding coupling constant. Here, the self-energy insertion has caused the bare velocity v to be replaced by the renormalized, scale-dependent velocity v_q. The second term J is a dimensionless function representing the combined effects of self-energy and vertex corrections beyond the simple rescaling of v. In the notation of Sodemann and Fogler, J is given by $J(x) \equiv I_a(ix) + I_b(ix)$, where the functions I_a and I_b, defined in Ref. [35], are analytically continued here to the imaginary x axis. It is essential to our subsequent arguments that $J(x)$ is a smooth function of x, varying monotonically between $J(0) \approx 0.497$ and $J(x \to \infty) \approx (0.013/x) \equiv (C_\infty/x)$. [See Eq. (12) and Fig. 2, where a numerical fit to $J(x)$ is provided.] This feature is expected to persist beyond the first-order approximation, e.g., even in the strong-coupling limit, where the renormalized velocity is likely given by $v_q^{(2)}$ of Eq. (5) (see Ref. [24]). A simple fit to $J(x)$ based on the results of Ref. [35] is

$$J(x) = \frac{(y + a)J(0) + (y^3 - 1)aC_\infty}{y^3(1 + ay)}, \tag{12}$$

where $a = 0.285$ and $y = \sqrt{1 + x^2}$. The function $J(x)$ is shown in Fig. 2. For imaginary x, this numerical fit provides a good match to the results of Ref. [35].

Substituting Eq. (11) into Eq. (9), we obtain the full interacting response function in the form

$$\chi(q, iu) = -\frac{q}{4\hbar v_q} \frac{1 + \alpha_q H(x_q)}{\sqrt{1 + x_q^2} + \frac{\pi}{2}\alpha_q [1 + \alpha_q H(x_q)]}, \tag{13}$$

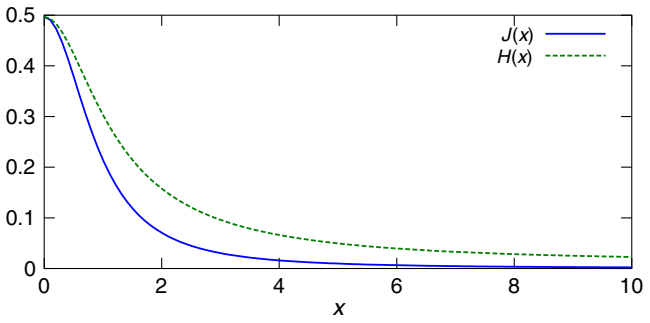

FIG. 2. Numerical fit [Eq. (12)] to the functions $J(x)$ (solid line) and $H(x) \equiv J(x)\sqrt{1 + x^2}$ (dashed line) that control the magnitude of the self-energy and vertex corrections to the RPA beyond the simple renormalization of the velocity.

where $H(x) \equiv J(x)\sqrt{1+x^2}$. Plugging into Eq. (8) and changing the integration variable from q to $\bar{q} = 2qD$, we find, after simple manipulations,

$$\frac{E^{(2)}}{A} = -\frac{e^2}{32\pi D^3}\int_0^\infty \frac{1}{2}\bar{q}^2 e^{-\bar{q}}\tilde{F}\left(\frac{\pi}{2}\alpha_{\bar{q}/2D}\right)d\bar{q}, \qquad (14)$$

where we have defined the function

$$\tilde{F}(a) \equiv a\int_0^\infty \left\{\frac{1+\frac{2a}{\pi}H(x)}{\sqrt{1+x^2}+a[1+\frac{2a}{\pi}H(x)]}\right\}^2 dx. \qquad (15)$$

If now self-energy and vertex corrections are neglected by setting $H = 0$, we see that $\tilde{F}$ simplifies to

$$F(a) \equiv a\int_0^\infty \left\{\frac{1}{\sqrt{1+x^2}+a}\right\}^2 dx, \qquad (16)$$

which can be evaluated analytically, yielding

$$F(a) = \begin{cases} \frac{\frac{a\pi}{2} - a^2\sqrt{1-a^2} - a\tan^{-1}\left(\frac{a}{\sqrt{1-a^2}}\right)}{(1-a^2)^{3/2}} & a < 1 \\ \frac{a^2 - \frac{a}{2\sqrt{a^2-1}}\log\frac{a+\sqrt{a^2-1}}{a-\sqrt{a^2-1}}}{(a^2-1)} & a > 1 \end{cases} \qquad (17)$$

and $F(a) = 2/3$ for $a = 1$. Equation (17) is precisely the function F that was introduced in Eq. (3) and was plotted in Fig. 1. Since, in RPA, α_q is constant ($\alpha_q = \alpha$) and $\int_0^\infty \bar{q}^2 e^{-\bar{q}} d\bar{q} = 2$, Eq. (3) is seen to follow immediately from Eq. (14).

To go beyond the RPA, we must reinstate the self-energy and the vertex corrections. However, we observe that in the large-D limit, the coupling constant tends to 0, and therefore, the $\tilde{F}$ function reduces to the F function, which in turn can be replaced by its small-a expansion $F(a) \approx (\pi/2)a$. Thus, Eq. (14) becomes

$$\frac{E^{(2)}}{A} = -\frac{\pi e^2}{256 D^3}\int_0^\infty \bar{q}^2 e^{-\bar{q}}\alpha_{\bar{q}/2D} d\bar{q}. \qquad (18)$$

The asymptotic behavior of the vdW interaction depends solely on the behavior of the running coupling constant α_q (or, equivalently, the renormalized velocity) in the $q \to 0$ limit. For the logarithmic renormalization case of Eq. (4), we evaluate Eq. (18) by freezing the slowly varying $\alpha^{(1)}_{q/2D}$, evaluating it at the maximizing value $q_0 = 2$ of the rapidly varying integrand, getting

$$\frac{E^{(2)}}{A} \approx -\frac{\pi e^2}{128 D^3}\left[\frac{\alpha}{1+\frac{1}{4}\alpha\ln(\Lambda D)}\right]. \qquad (19)$$

Equation (19) shows a modest, logarithmic reduction of the vdW interaction relative to the RPA result. If, on the other hand, the strong-coupling model of Eq. (5) is adopted, Eq. (18) gives an altogether different power-law behavior:

$$\frac{E^{(2)}}{A} = -\frac{\pi\Gamma(3+\beta)\Lambda^\beta e^2}{32(2D)^{3+\beta}}, \qquad (20)$$

where $\Gamma(x)$ is the gamma function. Notice that, since $\beta < 1$, Eq. (20) is still larger than the D^{-4} dependence expected for insulating 2D layers and therefore dominates at large separations in real graphene, where gapped insulator-type transitions also contribute to the response.

The above Eqs. (18)–(20) are valid at asymptotically large separations. At finite separations, the more accurate Eqs. (14) and (15) must be used. Equations (14) and (15) now depend not only on the fermion velocity—a measurable quantity—but also on the form of the function $J(x)$, which is not directly accessible to experiment and must be calculated by many-body theory. (Notice, however, that the imaginary part of the density response function for the real frequency is related to the optical absorption spectrum, which is, in principle, measurable, and could be used to calculate the function J.) Making use of $J(x)$ calculated in Ref. [35] and fitted as shown in Fig. 2, we find that

$$\tilde{F}(a) \approx \left(1 + 0.165\frac{(2.1a)}{\sqrt{1+(2.1a)^2}}\right)F(a) \qquad (21)$$

is an excellent approximation (relative error under 1%) to the integral of Eq. (15). Using Eq. (21) in Eq. (14), together with Eq. (4) or Eq. (5) for the velocity, we find that the distance dependence in the intermediate regime is basically D^{-3} with only a modest further dependence on distance via $F((\pi/2)\alpha_{q=1/D})$ or $\tilde{F}((\pi/2)\alpha_{q=1/D})$ [38].

In Fig. 3, we plot the force and its local exponent (in $F \propto D^{-p(D)}$) for the RPA energy $E^{(2)}_{\mathrm{RPA}}/A = -e^2/(32\pi D^3)F(\alpha)$ and the vdW interaction calculated through Eq. (14) using Eqs. (4) and (5). Using the stretched graphite vdW energy formula of Refs. [11,39] yields remarkably similar results for the equivalent in bulk graphite (up to a constant). Naturally, the situation differs between the weak-coupling [Eq. (4)] and strong-coupling [Eq. (5)] models of the renormalized velocity. The interaction energy and force are qualitatively different from the RPA at large separations and show moderate quantitative differences at intermediate separations, less than 25% for $D < 100$ Å. Observation of such deviations from the RPA will provide additional evidence of the many-body renormalization of the fermion velocity. We note that for intermediate values of D ($D \lesssim 20$ nm), further modifications are required even at the RPA level to account for departures of the graphene electronic band structure from a perfect infinite cone [11] or anisotropy [12].

There have been some proposals (see Ref. [24] and references therein) that strong coupling could bring excitonic effects, leading to a gap. In that case, the vdW energy

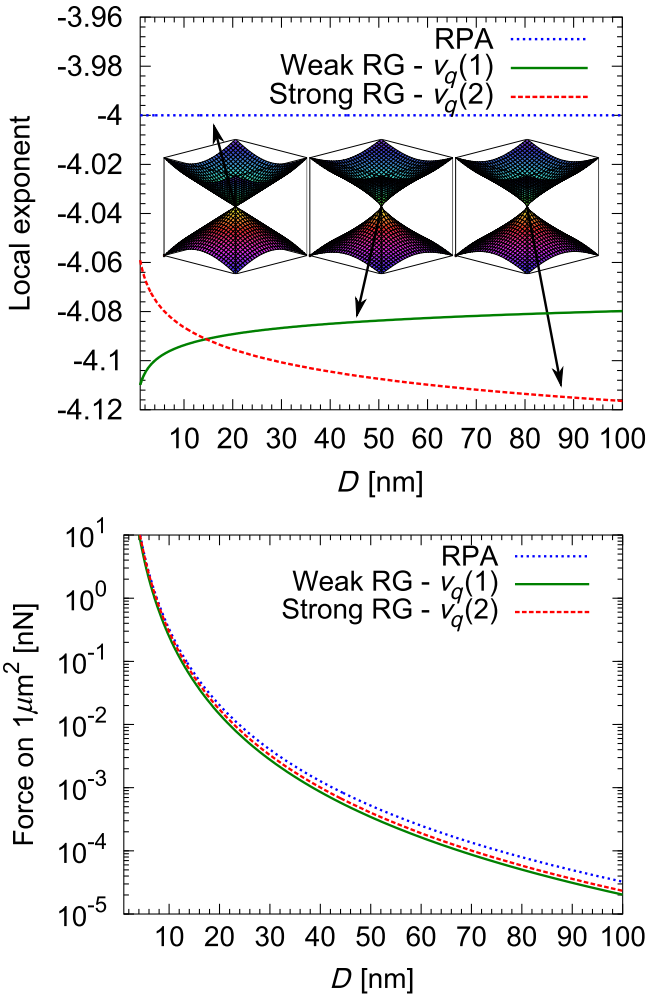

FIG. 3. Plot of the local exponent $p(D) = (d\log|F|/d\log D)$ of the force (top, with band-structure inset) and the force $F = (dE^{(2)}/dD)$ (bottom) using the RPA (dotted line), $v_q^{(1)}$ [Eq. (4), solid line], and $v_q^{(2)}$ [Eq. (5), with $\beta = 2/\pi^2$, dashed line]. Here, we fix $v = 10^5$ m/s and $\Lambda = 1/(1.42\ \text{Å})$.

might show the insulating D^{-4} behavior as in Eq. (1). There seems to be little experimental evidence so far that graphene can be an excitonic insulator, however.

IV. EXPERIMENTAL OPTIONS

While our paper, in the main, concerns the theory of the renormalization of the vdW interaction, it serves as one of several motivating factors for a renewed experimental effort for direct measurement of the vdW forces on high-quality graphene flakes. These measurements would also be needed to resolve existing controversies about graphitic cohesion, in general. In this section, we briefly discuss the current prospects for such measurements, and we hope thereby to stimulate experimentalists in this direction.

While there have been a number of experiments [40–43] that have indirectly determined the binding energy of graphene planes, these experiments have produced a wide range of results, and most have relied on questionable theoretical assumptions for their analysis, so that the whole field is somewhat controversial [44]. Purely theoretical estimates have also varied widely [3,14,16,45–51], although recent very large and relatively high-level (RPA [16] and diffusion Monte Carlo [49]) calculations are starting to show consistency. These same high-level types of theory also predict the forces between nanostructures such as graphene planes as a function of distance, showing very different results from popular pairwise-additive-force theories, in the asymptotic region of large separations [see Eqs. (2) and (6)].

The force between graphenes at such asymptotic distances does not appear to have been measured at all so far. In view of this fact, as well as the aforementioned binding-energy controversies, direct measurement of such forces at all distances would be very desirable. As the distant forces are relatively small, atomic force microscopy or a related nano electro mechanical oscillator approach would be the preferred route. For the basic RPA analysis of two cold undoped-graphene sheets of lateral dimension one micron, separated by 10 nm, the predicted force is a few nanonewtons, well within AFM capabilities, with larger forces for larger flake areas.

In the ideal case analyzed in the main text, there are two freestanding undoped-graphene sheets at a temperature below 10 K. Single sheets of high-quality graphene have certainly been subjected to various measurements [52], and vdW forces due to a single supported graphene sheet have been seen [53], but force experiments with two freestanding sheets are rare or absent and will require some effort to ensure a reasonable degree of parallelism.

Perhaps a better short-term prospect is, therefore, to measure the force between a single freestanding sheet and its own "vdW image" in the surface of a bulk metallic substrate. A very recent related experiment, using a metal grating instead of graphene and an $O(100\text{-}\mu\text{m})$-radius gold sphere as the substrate to avoid parallelism issues, has been highly successful [54]. This experiment also demonstrated the use of colocated fiber optics for precise control of the separation D down to < 200 nm. The theory of this geometry will be analyzed in detail elsewhere but is expected [see Eq. (A7)] to yield similar predictions to the ones in the main text.

The unavoidable corrugation of the freestanding graphene sheets should not be a problem, as it is known experimentally not to affect electronic properties substantially and would only contribute a very few-percent uncertainty in the separation D between the sheets, at the separations of a few tens to hundreds of nanometers that are relevant to the main text. This uncertainty would not affect the analysis of the force power law proposed in the text, as one would aim for measurements at D values spanning an order of magnitude.

A more subtle problem is the likely existence of metallic n- and p-type "puddles" on the undoped sheets [55]. Provided that the sheets are of sufficient quality that the puddles are disconnected objects of the typical spatial extent λ, we predict that they contribute an "insulatorlike" vdW interaction energy varying with distance D as $(\text{const})D^{-4}$ when $D > \lambda$, clearly distinguishable from the lower powers predicted in the text, arising from the undoped nonpuddle areas. Recent experiments [55] suggest that $\lambda = O(1\ \text{nm})$, so that force experiments at $D = O(10\text{–}200\ \text{nm})$ would still exhibit undoped-graphene properties.

Another experimental route would be to avoid separating the sheets in their perpendicular direction but rather to slide them off one another in a surface-parallel direction. This task may be easier experimentally because of the recent centrifugation-based preparation of high-quality micron-sized stacks of 2–5 graphene monolayers [56]. These layers are spatially staggered like a slipped deck of cards, potentially allowing the attachment of an AFM tip to the projecting edges of individual sheets. The force during the entire lateral sliding process, out to wide separation into disjunct coplanar sheets, would be measured. The noncontact part of this force can be expected to show effects from the coupling of long-wavelength electronic charge fluctuations and hence renormalization effects in the graphene polarizability, just as for the case of parallel sheets separated by distance D measured perpendicular to the sheets. From the theory point of view, the analysis of this geometry is more difficult and has not yet been attempted in detail.

A further possibility for measurement might come from modifying the experiment of Tautz [57] in which aromatic molecules were pulled off a metal surface by an AFM tip, although, once again, the theory would need modification for this geometry.

The above considerations suggest that it will be possible to achieve a much-improved understanding of graphenic cohesive forces by direct measurement. It might be interesting to seek similar anomalous vdW effects between thin films of 3D topological insulators [58] and between low-dimensional strongly correlated systems, in general.

V. CONCLUSION

In conclusion, we have shown that the low-temperature dispersion (vdW) interaction between two infinite parallel nondoped-graphene sheets is significantly modified by many-body effects beyond the RPA. Not only is the interaction quantitatively reduced, but also, its qualitative asymptotic behavior is modified. The main source of the effect is the many-body renormalization of the velocity of the massless Dirac fermions. This renormalization has been the subject of many recent investigations [17–21]. It is experimentally observed as a deformation of the Dirac cones near the point of contact. Our findings demonstrate that the same renormalization manifests itself in the long-distance behavior of the dispersion forces.

Direct measurement of the asymptotic graphene-graphene vdW interaction could therefore distinguish between much-debated theory models of electrons in graphene—weak renormalization [Eq. (19)], strong renormalization [Eq. (20)], and excitonic insulator [Eq. (1)]. Such experiments in the asymptotic vdW region will be demanding, but we estimate, e.g., a measurable force of order nN (see the lower panel of Fig. 3) between micron-sized graphene sheets separated by $O(10\ \text{nm})$. Observation of the vdW image force in a metal substrate could avoid the need for two graphene sheets, and there are other possibilities, too. (See Ref. [56] and the second-to-last paragraph of Sec. IV above.) Very recent experiments [54] support the general feasibility of our proposals. We estimate that complications due to graphene wrinkling and puddling [55] will not destroy our effect. Indeed, the time is ripe for direct force measurements to clarify this controversy and other recent controversies [44] over graphenic cohesion, in general.

ACKNOWLEDGMENTS

T. G. and J. F. D. were supported by Australian Research Council Grant No. DP1096240. G. V. was supported by NSF Grant No. DMR-1104788. J. F. D. appreciates hospitality at the University of Missouri, the Donostia International Physics Centre, and the European Theoretical Spectroscopy Facility.

APPENDIX: VAN DER WAALS FORCE BETWEEN GRAPHENE AND A METAL BULK

Here, we investigate the van der Waals force between a single graphene layer and a metal bulk, which may be more appropriate for likely successful experimental arrangements (see Sec. IV). We predict that it will obey the same overall power law as the response between two graphene layers, with at most a logarithmic correction (as a function of D). Similarly, the dependence on the many-body beyond-RPA effects is expected to be maintained. Here we offer evidence that these predictions are valid.

We make use of the relationship [59]

$$\frac{E_{\text{vdW}}}{A} = \frac{\hbar}{8\pi^3}\int d^2\vec{q}\int_0^\infty du\,\log(1-\zeta) \tag{A1}$$

$$\approx -\frac{\hbar}{8\pi^3}\int d^2\vec{q}\int_0^\infty du\zeta \tag{A2}$$

for the van der Waals potential between semi-infinite bulks and layers interacting across a single surface. In the case of a layer of graphene interacting with a bulk metal,

$$\zeta = e^{-2qD}\frac{2\pi e^2}{q}\chi_{\mathrm{Gr}}(q,iu) \times \frac{2\pi e^2}{q}\int dz dz' e^{-q|z+z'|}\chi_{\mathrm{metal}}(q,z,z',iu) \quad \text{(A3)}$$

$$\equiv C_{\mathrm{Gr}}(q,iu)C_{\mathrm{metal}}(iu)e^{-2qD}, \quad \text{(A4)}$$

where $\chi_{\mathrm{Gr}}(q,iu)$ is the interacting response of the graphene layer and χ_{metal} is the bulk response of the metal. Here, $C_{\mathrm{metal}} = (\epsilon(iu)-1)/(\epsilon(iu)+1)$, where $\epsilon \approx 1+(\omega_p^2/u^2)$ is the dielectric function of the metal.

From Eqs. (9) and (13), we see that $C_{\mathrm{Gr}} \equiv (-2\pi e^2/q)\chi_{\mathrm{Gr}}(q,iu)$ can be written as $C_{\mathrm{Gr}}(x,\alpha_q) \approx ((\pi\alpha_q/2)/(\sqrt{1+x^2}+\pi\alpha_q/2))$, where $x = u/(v_q q)$ and $\alpha_q = e^2/(\hbar v_q)$ varies slowly with q. Thus,

$$\frac{E_{\mathrm{vdW}}}{A} = \frac{e^2}{4\pi^2 D^3}\int \bar{q}^2 e^{-\bar{q}} d\bar{q}\int_0^\infty dx \times \frac{C_{\mathrm{Gr}}(x,\alpha_{\bar{q}/(2D)})}{\alpha_{\bar{q}(2D)}}\frac{1}{1+\frac{v_{\bar{q}/(2D)}^2\bar{q}^2}{2D^2\omega_p^2}x^2}, \quad \text{(A5)}$$

where we also use $\bar{q} = 2qD$. Clearly, the form of α_q will have a substantial effect on the asymptotic behavior of the vdW potential, similarly to the bigraphene case. Using $C_{\mathrm{Gr}} < ((\pi/2\alpha)/x + \pi/2\alpha)$ and setting $\alpha_{\bar{q}/2D} \approx \alpha_{1/D}$ give

$$\frac{E_{\mathrm{vdW}}}{A} < \frac{e^2}{4\pi^2 D^3}\int \bar{q}^2 e^{-\bar{q}} d\bar{q}\int_0^\infty dx \times \frac{\pi/2}{x+\pi/2\alpha_{1/D}}\frac{1}{1+\frac{v_{1/D}^2\bar{q}^2}{2D^2\omega_p^2}x^2} \quad \text{(A6)}$$

$$\approx \frac{\alpha_{1/D}\log(D/D_0)}{D^3}, \quad \text{(A7)}$$

where $D_0 \propto (e^2/\hbar\omega_p) = O(1\ \text{Å})$; i.e., the asymptotic interaction has an extra logarithmic term compared to the bigraphene case $k\alpha_{1/D}/D^3$. The prefactor $\alpha_{1/D}$ ensures that the difference between different renormalization scenarios is maintained.

One can, of course, perform the integral (A5) [or an equivalent expression for Eq. (A1)] numerically for a given graphene velocity v_q and dielectric frequency ω_p. However, the important asymptotic physics is clearer in the bigraphene case tested in the paper, and the deviation caused by the bulk metal is expected to be small at the $O(10\text{–}100\ \text{nm})$ distances we propose investigating.

[1] A. H. Castro Neto, F. Guinea, N. M. R. Peres, K. S. Novoselov, and A. K. Geim, *The Electronic Properties of Graphene*, Rev. Mod. Phys. **81**, 109 (2009).

[2] S. Grimme, *Semiempirical GGA-Type Density Functional Constructed with a Long-Range Dispersion Correction*, J. Comput. Chem. **27**, 1787 (2006).

[3] M. Dion, H. Rydberg, E. Schröder, D. C. Langreth, and B. I. Lundqvist, *van der Waals Density Functional for General Geometries*, Phys. Rev. Lett. **92**, 246401 (2004).

[4] D. C. Langreth, M. Dion, H. Rydberg, E. Schröder, P. Hyldgaard, and B. I. Lundqvist, *van der Waals Density Functional Theory with Applications*, Int. J. Quantum Chem. **101**, 599 (2005).

[5] A. Tkatchenko and M. Scheffler, *Accurate Molecular van der Waals Interactions from Ground-State Electron Density and Free-Atom Reference Data*, Phys. Rev. Lett. **102**, 073005 (2009).

[6] O. A. Vydrov and T. Van Voorhis, *Dispersion Interactions from a Local Polarizability Model*, Phys. Rev. A **81**, 062708 (2010).

[7] J. F. Dobson and T. Gould, *Calculation of Dispersion Energies*, J. Phys. Condens. Matter **24**, 073201 (2012).

[8] J. F. Dobson, A. White, and A. Rubio, *Asymptotics of the Dispersion Interaction: Analytic Benchmarks for van der Waals Energy Functionals*, Phys. Rev. Lett. **96**, 073201 (2006); note that χ_0 in this work was too large by a factor of 2.

[9] T. Gould, K. Simpkins, and J. F. Dobson, *Theoretical and Semiempirical Correction to the Long-Range Dispersion Power Law of Stretched Graphite*, Phys. Rev. B **77**, 165134 (2008).

[10] Bo E. Sernelius, *Graphene as a Strictly 2D Sheet or as a Film of Small but Finite Thickness*, Graphene **01**, 21 (2012).

[11] T. Gould, J. F. Dobson, and S. Lebègue, *Effects of a Finite Dirac Cone on the Dispersion Properties of Graphite*, Phys. Rev. B **87**, 165422 (2013).

[12] A. Sharma, P. Harnish, A. Sylvester, V. N. Kotov, and A. H. Castro Neto, *van der Waals Forces and Electron-Electron Interactions in Two Strained Graphene Layers*, arXiv:1402.3369.

[13] V. V. Gobre and A. Tkatchenko, *Scaling Laws for van der Waals Interactions in Nanostructured Materials*, Nat. Commun. **4**, 2341 (2013).

[14] D. Drosdoff and L. M. Woods, *Casimir Forces and Graphene Sheets*, Phys. Rev. B **82**, 155459 (2010).

[15] D. Drosdoff, A. D. Phan, L. M. Woods, I. V. Bondarev, and J. F. Dobson, *Effects of Spatial Dispersion on the Casimir Force between Graphene Sheets*, Eur. Phys. J. B **85**, 1 (2012).

[16] S. Lebègue, J. Harl, T. Gould, J. G. Ángyán, G. Kresse, and J. F. Dobson, *Cohesive Properties and Asymptotics of the Dispersion Interaction in Graphite by the Random Phase Approximation*, Phys. Rev. Lett. **105**, 196401 (2010).

[17] J. González, F. Guinea, and M. A. H. Vozmediano, *Non-Fermi Liquid Behavior of Electrons in the Half-Filled Honeycomb Lattice (A Renormalization Group Approach)*, Nucl. Phys. **B424**, 595 (1994).

[18] J. González, F. Guinea, and M. A. H. Vozmediano, *Marginal-Fermi-Liquid Behavior from Two-Dimensional Coulomb Interaction*, Phys. Rev. B **59**, R2474 (1999).

[19] Z. Q. Li, E. A. Henriksen, Z. Jiang, Z. Hao, M. C. Martin, P. Kim, H. L. Stormer, and D. N. Basov, *Dirac Charge Dynamics in Graphene by Infrared Spectroscopy*, Nat. Phys. **4**, 532 (2008).

[20] D. C. Elias, R. V. Gorbachev, A. S. Mayorov, S. V. Morozov, A. A. Zhukov, P. Blake, L. A. Ponomarenko, I. V. Grigorieva, K. S. Novoselov, F. Guinea, and A. K. Geim, *Dirac Cones Reshaped by Interaction Effects in Suspended Graphene*, Nat. Phys. **7**, 701 (2011).

[21] D. A. Siegel, C.-H. Park, C. Hwang, J. Deslippe, A. V. Fedorov, S. G. Louie, and A. Lanzara, *Many-Body Interactions in Quasi-freestanding Graphene*, Proc. Natl. Acad. Sci. U.S.A. **108**, 11 365 (2011).

[22] I. F. Herbut, *Interactions, and Phase Transitions on Graphene's Honeycomb Lattice*, Phys. Rev. Lett. **97**, 146401 (2006).

[23] E. G. Mishchenko, *Dynamic Conductivity in Graphene beyond Linear Response*, Phys. Rev. Lett. **103**, 246802 (2009).

[24] V. N. Kotov, B. Uchoa, V. M. Pereira, F. Guinea, and A. H. Castro Neto, *Electron-Electron Interactions in Graphene: Current Status and Perspectives*, Rev. Mod. Phys. **84**, 1067 (2012).

[25] T. Olsen and K. S. Thygesen, *Extending the Random-Phase Approximation for Electronic Correlation Energies: The Renormalized Adiabatic Local Density Approximation*, Phys. Rev. B **86**, 081103 (2012).

[26] T. Olsen and K. S. Thygesen, *Beyond the Random Phase Approximation: Improved Description of Short Range Correlation by a Renormalized Adiabatic Local Density Approximation*, arXiv:1306.2732.

[27] M. Polini, R. Asgari, Y. Barlas, T. Pereg-Barnea, and A. H. MacDonald, *Graphene: A Pseudochiral Fermi Liquid*, Solid State Commun. **143**, 58 (2007).

[28] S. Das Sarma, E. H. Hwang, and Wang-Kong Tse, *Many-Body Interaction Effects in Doped and Undoped Graphene: Fermi Liquid versus Non-Fermi Liquid*, Phys. Rev. B **75**, 121406 (2007).

[29] D. T. Son, *Quantum Critical Point in Graphene Approached in the Limit of Infinitely Strong Coulomb Interaction*, Phys. Rev. B **75**, 235423 (2007).

[30] M. S. Foster and I. L. Aleiner, *Graphene via Large n: A Renormalization Group Study*, Phys. Rev. B **77**, 195413 (2008).

[31] V. N. Kotov, B. Uchoa, and A. H. Castro Neto, $1/n$ *Expansion in Correlated Graphene*, Phys. Rev. B **80**, 165424 (2009).

[32] J. P. Reed, B. Uchoa, Y. Il Joe, Y. Gan, D. Casa, E. Fradkin, and P. Abbamonte, *The Effective Fine-Structure Constant of Freestanding Graphene Measured in Graphite*, Science **330**, 805 (2010).

[33] S. H. Abedinpour, G. Vignale, A. Principi, M. Polini, W.-K. Tse, and A. H. MacDonald, *Drude Weight, Plasmon Dispersion, and ac Conductivity in Doped Graphene Sheets*, Phys. Rev. B **84**, 045429 (2011).

[34] L. S. Levitov, A. V. Shtyk, and M. V. Feigelman, *Electron-Electron Interactions and Plasmon Dispersion in Graphene*, Phys. Rev. B **88**, 235403 (2013).

[35] I. Sodemann and M. M. Fogler, *Interaction Corrections to the Polarization Function of Graphene*, Phys. Rev. B **86**, 115408 (2012).

[36] G. F. Giuliani and G. Vignale, *Quantum Theory of the Electron Liquid* (Cambridge University Press, Cambridge, England, 2005).

[37] B. Wunsch, T. Stauber, F. Sols, and F. Guinea, *Dynamical Polarization of Graphene at Finite Doping*, New J. Phys. **8**, 318 (2006).

[38] Some care must be exerted when evaluating Eq. (14), as the asymptotic renormalized perturbation approach for the corrections is not fully appropriate for larger q. In particular, expression (4) is invalid for large q, as v_q can become negative. In our calculations, we use instead $\alpha'_q = e^2/(\hbar \max[v, v_q])$ to avoid unphysical results.

[39] T. Gould, E. Gray, and J. F. Dobson, *van der Waals Dispersion Power Laws for Cleavage, Exfoliation, and Stretching in Multiscale, Layered Systems*, Phys. Rev. B **79**, 113402 (2009).

[40] L. A. Girifalco and R. A. Lad, *Energy of Cohesion, Compressibility, and the Potential Energy Functions of the Graphite System*, J. Chem. Phys. **25**, 693 (1956).

[41] L. X. Benedict, N. G. Chopra, M. L. Cohen, A. Zettl, S. G. Louie, and V. H. Crespi, *Microscopic Determination of the Interlayer Binding Energy in Graphite*, Chem. Phys. Lett. **286**, 490 (1998).

[42] R. Zacharia, H. Ulbricht, and T. Hertel, *Interlayer Cohesive Energy of Graphite from Thermal Desorption of Polyaromatic Hydrocarbons*, Phys. Rev. B **69**, 155406 (2004).

[43] Z. Liu, J. Z. Liu, Y. Cheng, Z. Li, L. Wang, and Q. Zheng, *Interlayer Binding Energy of Graphite: A Mesoscopic Determination from Deformation*, Phys. Rev. B **85**, 205418 (2012).

[44] T. Gould, Z. Liu, J. Z. Liu, J. F. Dobson, Q. Zheng, and S. Lebègue, *Binding and Interlayer Force in the Near-Contact Region of Two Graphite Slabs: Experiment and Theory*, J. Chem. Phys. **139**, 224704 (2013).

[45] M. Hasegawa and K. Nishidate, *Semiempirical Approach to the Energetics of Interlayer Binding in Graphite*, Phys. Rev. B **70**, 205431 (2004).

[46] S. D. Chakarova-Käck, E. Schröder, B. I. Lundqvist, and D. C. Langreth, *Application of van der Waals Density Functional to an Extended System: Adsorption of Benzene and Naphthalene on Graphite*, Phys. Rev. Lett. **96**, 146107 (2006).

[47] E. Ziambaras, J. Kleis, E. Schröder, and P. Hyldgaard, *Potassium Intercalation in Graphite: A van der Waals Density-Functional Study*, Phys. Rev. B **76**, 155425 (2007).

[48] M. Hasegawa, K. Nishidate, and H. Iyetomi, *Energetics of Interlayer Binding in Graphite: The Semiempirical Approach Revisited*, Phys. Rev. B **76**, 115424 (2007).

[49] L. Spanu, S. Sorella, and G. Galli, *Nature and Strength of Interlayer Binding in Graphite*, Phys. Rev. Lett. **103**, 196401 (2009).

[50] J. D. Thrower, E. E. Friis, A. L. Skov, L. Nilsson, M. Andersen, L. Ferrighi, B. Jørgensen, S. Baouche, R. Balog, B. Hammer, and L. Hornekær, *Interaction between Coronene and Graphite from Temperature-Programmed Desorption and DFT-vdW Calculations: Importance of Entropic Effects and Insights into Graphite Interlayer Binding*, J. Phys. Chem. C **117**, 13520 (2013).

[51] T. Bučko, S. Lebègue, J. Hafner, and J. G. Ángyán, *Tkatchenko-Scheffler van der Waals Correction Method with and without Self-Consistent Screening Applied to Solids*, Phys. Rev. B **87**, 064110 (2013).

[52] K. R. Knox, A. Locatelli, M. B. Yilmaz, D. Cvetko, T. O. Menteş, M. Á. Niño, P. Kim, A. Morgante, and R. M. Osgood, *Making Angle-Resolved Photoemission Measurements on Corrugated Monolayer Crystals: Suspended Exfoliated Single-Crystal Graphene*, Phys. Rev. B **84**, 115401 (2011).

[53] A. A. Banishev, H. Wen, J. Xu, R. K. Kawakami, G. L. Klimchitskaya, V. M. Mostepanenko, and U. Mohideen, *Measuring the Casimir Force Gradient from Graphene on a* SiO_2 *Substrate*, Phys. Rev. B **87**, 205433 (2013).

[54] F. Intravaia, S. Koev, I. W. Jung, A. A. Talin, P. S. Davids, R. S. Decca, V. A. Aksyuk, D. A. R. Dalvit, and D. López, *Strong Casimir Force Reduction through Metallic Surface Nanostructuring*, Nat. Commun. **4**, 2515 (2013).

[55] S.-g. Cheng, H. Zhang, and Q.-f. Sun, *Effect of Electron-Hole Inhomogeneity on Specular Andreev Reflection and Andreev Retroreflection in a Graphene-Superconductor Hybrid System*, Phys. Rev. B **83**, 235403 (2011).

[56] X. Chen, J. F. Dobson, and C. L. Raston, *Vortex Fluidic Exfoliation of Graphite and Boron Nitride*, Chem. Commun. (Cambridge) **48**, 3703 (2012).

[57] S. Tautz, *Non-additivity of Molecule-Surface van der Waals Potentials from Force Measurements*, Bull. Am. Phys. Soc. **59**, G31.0001 (2014).

[58] J. J. Lee, F. T. Schmitt, R. G. Moore, I. M. Vishik, Y. Ma, and Z. X. Shen, *Intrinsic Ultrathin Topological Insulators Grown via Molecular Beam Epitaxy Characterized by In-Situ Angle Resolved Photoemission Spectroscopy*, Appl. Phys. Lett. **101**, 013118 (2012).

[59] J. F. Dobson, *Validity Comparison between Asymptotic Dispersion Energy Formalisms for Nanomaterials*, J. Comput. Theor. Nanosci. **6**, 960 (2009).